

Concrete defect identification and measurement in buildings

Maria Teresa Calcagni¹, Giovanni Salerno¹, Milena Martarelli¹, Jonas Urs Schlenger², Thomas Hassan³, Rene Heinikainen⁴, André Borrmann², Bruno Fies⁵, Gian Marco Revel¹

¹ Department of Industrial Engineering and Mathematical Sciences, Università Politecnica delle Marche, Via Breccia Bianche 12, 60131, Italy

² Chair of Computational Modeling and Simulation, Technical University of Munich, Arcisstraße 21, 80333, Germany

³ Orange, Rue Olivier de Serres 78, 75015, France

⁴ Fira Group Oy, Teknobulevardi 3-5, 01530, Finland

⁵ Centre Scientifique et Technique du Batiment, Avenue Jean Jaures 84, 77420, France

ABSTRACT

Ensuring the durability of civil buildings is critical for preventing long-term structural failure. Traditional damage assessment methods, based on visual inspections, are labour-intensive and subjective. The adoption of digital platforms emerges as a solution for complete monitoring of a building during its life cycle. This study, carried out as part of the European BIM2TWIN project, focuses on the monitoring of concrete surface quality using vision techniques and deep learning algorithms. Four neural network models are employed for cracks, honeycombing, pitting, and exposed bars, collectively analysing the images to identify and quantify defects. Project managers can assess the criticality of defects based on accurate pixel counts and geometric features, converting measurements from pixels to millimetres. Data is then stored in the digital platform, providing a historical record for future reference and decision-making by project managers.

Section: RESEARCH PAPER

Keywords: digital platform; concrete defects; identification; measurement; AI-algorithm

Citation: M. T. Calcagni, G. Salerno, M. Martarelli, J. U. Schlenger, T. Hassan, R. Heinikainen, A. Borrmann, B. Fies, G. M. Revel, Concrete defect identification and measurement in buildings, Acta IMEKO, vol. 14 (2025) no. 3, pp. 1-11. DOI: [10.21014/actaimeko.v14i3.1965](https://doi.org/10.21014/actaimeko.v14i3.1965)

Section Editor: Francesco Lamonaca, University of Calabria, Italy

Received October 30, 2024; **In final form** August 25, 2025; **Published** September 2025

Copyright: This is an open-access article distributed under the terms of the Creative Commons Attribution 3.0 License, which permits unrestricted use, distribution, and reproduction in any medium, provided the original author and source are credited.

Corresponding author: Maria Teresa Calcagni, e-mail: m.t.calcagni@pm.univpm.it

1. INTRODUCTION

Traditionally, security inspections involve a detailed visual examination of facilities by experienced inspectors. Although it is standard practice, manual observation is time-consuming and labour-intensive [1]. The greatest strength of manual visual inspection is hampered by a serious labour shortage: often, the number of qualified engineers is not enough for the number of buildings. If inspections are not carried out in time, uncontrollable deterioration of buildings may occur.

Therefore, an automated system or procedure based on image collection and processing, using Artificial Intelligence (AI) and computer vision techniques, could offer an ingenious solution in terms of maintenance practice. Kohoutek states that early applications of AI in instrumentation suggest that the existing quality management framework can effectively address the challenges posed by intelligent systems [2]. An example is proposed in [3], where a Heritage Building Information Model (HBIM) system that consolidates all archival information into a

single digital platform, enriched with data that can be consulted, analysed and updated, is presented. In fact, monitoring the building during its life cycle can improve productivity, resource efficiency, health and safety in building environments [4]. Over the years, several methods have been demonstrated to investigate and detect the defects in concrete surfaces. Zhang et al. used acoustic emission and Computed Tomography (CT) techniques for concrete cracking behaviour analysis [5], Hong et al. demonstrated a combination of Digital Image Correlation (DIC) and passive Infrared Thermography (IRT) for the detection and evaluation of defects [6]. Recently, vision systems have become more widespread, and scientific studies and applications have begun to move in this direction, combining vision systems and AI algorithms. The quality inspection system described by Rodriguez et al. is based on in-field image acquisition and processing for defect localization and detection. Defect localization is performed by means of image segmentation, and defect recognition is carried out by means of neural networks [7].

Machine learning technology has allowed time consuming inspection procedures to speed up and become applicable in daily routines. Some types of defects that may also occur during the construction phase are described in [8].

In [9], an automated system is presented; it is based on the collection and processing of multiple images taken from a distance, using different camera poses. This study is focused on the defect detection of the textural surfaces of buildings.

The research proposes a method for identifying and measuring surface defects in buildings under construction, developing an algorithm and a system that balances portability and accuracy, based on proprietary data and Non-Destructive Testing (NDT) to improve inspection and repair. In a recent study, an innovative video processing method was used to detect early warning signals before the structural collapse of historic masonry during seismic tests [10]. The integration of an early warning system with the non-destructive monitoring approach discussed in Section 3 could provide early warnings and allow for eventual correction.

The state-of-the-art analysis is described in detail in Section 2. The inspection tool for concrete surface quality control and the design for its integration into the digital platform (a web-based structural software that speeds and simplifies communication between users) are described in Section 3. Section 4 presents an application use case, Section 5 reports the discussion followed by the conclusions in Section 6.

2. STATE-OF-THE-ART ANALYSIS

Human inspection is prevalent today, but several methods are being investigated to find a more automatic and less time-consuming method of defect detection [11].

Several inspection methods have been investigated recently. Techniques to study how defects affect the failure behaviour of concrete were inspected, demonstrating that internal cavities reduce strength and deformation properties.

A method developed by Chow et al. aims to detect concrete surface anomalies, and extract and classify the defects using deep learning classifiers [12]. A structured dataset combined with deep learning techniques and transfer learning [13] was used for defects identification on a conventional bridge.

For defect detection in concrete surfaces, with the goal of overcoming the challenges faced by current image processing techniques (IPTs) in real-world scenarios with varying conditions, Wang et al. proposed a model using deep learning, a one-stage object detection network, with the EfficientNetB0 backbone network and a detector inspired by a pyramidal feature network [14]. AI-based systems were studied for the automatic detection of specific mechanical attributes of concrete and for crack detection [15]. Dang et al. propose a method for concrete defect investigation based on deep learning and present the components used for the case study [16].

In [17], different crack image datasets were used to train the network and evaluate their impact on model performance and address network domain limitations.

The importance of early defect detection to maintain the stability of concrete bridges is emphasized in [18], which proposes a hybrid network for defect classification consisting of a convolutional neural network, a Transformer, and an MLP (Multilayer Perceptron) head achieving good results.

An automated defect inspection using a 360° camera in combination with LiDAR (Light Detection and Ranging) is described in [19], where defect assessment was performed by

aligning images and depth data; these data were then entered into a BIM. Crack evaluation and detection were performed in [20] using deep learning and structured light.

The occurrence of a crack could be generated by the corrosion of the frame inside the concrete [21] or by structural damage that can result from natural disasters [22]. Cracks are damaging openings—Figure 1(a)—that appear in a structural element, developing throughout its depth. Concrete fissures are small cracks at the surface level, which mainly affect its finish, deteriorating the surface of the structural element [23].

Another type of concrete defect is pitting; it consists of small pits or indentations on the surface, see Figure 1(b). Pitting can undermine the overall structure of concrete and make it more prone to damage. It can also reduce the aesthetics of the concrete surface. These defects can be generated from freeze and thaw cycles, the corrosion of the reinforcing steel, and several other factors [24].

Concrete honeycombing is represented by cavities and voids on or within the surface, see Figure 1(c). The cause may be poor coverage, improper vibration and sometimes bleeding of concrete, erroneous concrete mixture, too much or not enough water, vibration process not managed correctly during casting, or a combination of the previous ones [25].

Exposed bars in concrete, as in Figure 1(d), appear in reinforced concrete structures. In fact, concrete deterioration may occur due to the improper mixture of cement, steel corrosion, and/or freeze and thaw cycles [26].

The system presented in this paper proposes an innovative algorithm for the detection, identification, and measurement of cracks, honeycombing, exposed bars and pitting, filling significant gaps in current state-of-the-art systems. Unlike existing solutions, which often cannot measure the size of the defects, our system not only identifies defects but also quantifies their size. This innovative service leverages AI intelligence models obtained by advanced machine learning and deep learning techniques, and it is enhanced by defect-adapted measurement algorithms and an appropriate combination of devices. To achieve this, a specific dataset was created to train the AI, resulting in a specialized model for each type of surface defect. By combining these four models, we ensure complete defect identification and recognition. Each defect was rigorously evaluated using the acquired information, facilitating an NDT approach to defect inspection and evaluation. Finally, the

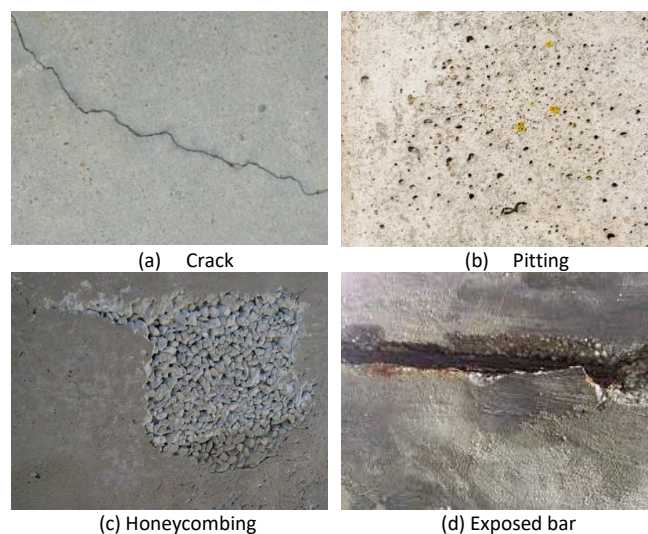


Figure 1. Concrete defects considered for this algorithm.

integration of tailored software and hardware led to the creation of a portable and user-friendly system that can operate effectively under any condition. This release highlights the innovative aspects of this work, particularly the way it addresses the shortcomings of current systems and the unique ability to identify and measure defects.

3. CONCRETE SURFACE QUALITY CONTROL

3.1. Concrete defect measurement system

The integrity of concrete surfaces in construction projects is a crucial concern, which can be improved by monitoring with vision sensors and advanced AI-based algorithms.

The images of defected areas are captured by the user using a visible camera and are analysed by the algorithms to automatically extract the identification of a (or several) defect type class, and the measurement of the features of interest.

3.1.1. Image acquisition system design

The vision-based measurement system consists of a combination of visible and depth cameras.

Visible cameras capture 2D RGB or grey-scale images, while depth cameras provide distance data extracted from the depth map, indicating the separation between the visual apparatus and the framed surface. 2D images can be obtained with various types of cameras, such as monochrome cameras, DSLR cameras or those embedded in mobile devices such as smartphones, tablets.

In this in-field use case (Section 4), the visible camera used is a Nikon D7200 [27], and the depth camera used is an Intel RealSense L515 LiDAR [28].

Features identification can be performed by using only visible images. On the other hand, if feature measurement must be performed, the depth data is needed, allowing the conversion from pixel to a dimensional unit. A calibration enables pixel-to-millimetres conversion, using the depth data and the focal length of the lens as input. The calibration procedure can be performed previously in the laboratory. During the building inspection the calibration can be avoided, and the user can expedite acquisitions. An example of a monitoring toolkit with a visible camera and a depth camera is shown in Figure 2.

When a construction phase is completed, e.g., after the pouring of concrete, the digital platform sends a notification message to the quality control manager, and the surface inspection can be executed.



Figure 2. A monitoring toolkit consisting of a visible camera and depth camera.

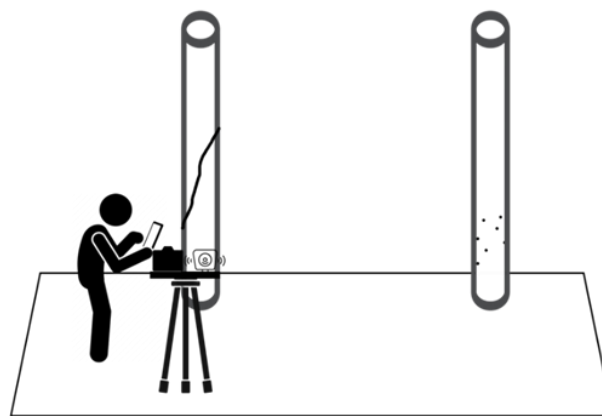


Figure 3. A monitoring toolkit installed in the field.

Images are captured and processed, and if a concrete surface defect is identified, the output of the quality control software is added to the digital platform.

A sketch of the measurement operation is given in Figure 3.

3.1.2. AI-based defect identification system

The AI-based defect identification system is designed to assign a given input image to one or more pre-defined defect categories. The system comprises four distinct models, each trained and specialised to identify a specific type of defect, the ones described in Figure 1.

The image is analysed by the four models, and the output (segmented image) is subsequently analysed by computer vision algorithms to measure the entity of the features of interest.

The architecture used in this implementation is U-Net [29], a neural network developed for precise image segmentation. Based on a fully convolutional neural network, it was first applied in the biomedical field for image segmentation [30]. Thanks to its performance and speed of execution, U-Net was selected for defect segmentation and recognition activities.

The U-Net architecture is composed of two symmetric parts: the encoding (or contracting) path and the decoding (or expanding) path. The encoding path consists of the repeated application of convolutions, followed by the activation of Rectified Linear Units (ReLU) and max pooling operations. This path is designed to abstract and compress spatial information, thus capturing the wider context of the image. Conversely, the decoding path includes uplinks that progressively increase the resolution of the abstracted features. This approach facilitates the detailed segmentation of objects at various scales.

The effectiveness of neural network models depends on the quality of the data used to train them. The selection of an appropriate dataset is crucial to ensure the creation of accurate and reliable models. A targeted dataset was created by collecting images from several instances: acquisition campaigns were conducted in ruined buildings around Ancona, Italy, and in Helsinki, Finland, during the construction of buildings by one of our partners, the construction company FIRA. The total amount of images for each category is as follows:

1. crack: 750,
2. pitting: 1320,
3. honeycombing: 640,
4. exposed bar: 400,

which was divided into training, validation, and test datasets following the ratio of 80 %, 10 %, 10 %.

In evaluating the performance of the U-Net architecture for segmentation tasks, two key metrics are considered: the

Intersection over Union (IoU) score and the model loss. The IoU score, also known as the Jaccard index, quantifies the accuracy of the expected segmentation. It is a widely accepted metric in the field of computer vision and image segmentation, and a higher IoU score indicates better segmentation performance. It is calculated as the area of overlap between the predicted segmentation and ground truth divided by the union area:

$$IoU = \frac{A \cap B}{A \cup B} = \frac{TP}{TP + FP + FN} \quad (1)$$

with

TP: True Positives

FP: False Positives

FN: False Negatives

$A \cap B$: Area of Overlap

$A \cup B$: Area of Union

For model loss, a combination of Dice Loss and Focal Loss was used to optimise the segmentation results. Dice Loss is a function that measures the similarity between the predicted segmentation and ground truth and is therefore particularly effective for managing class imbalance in images [31]. On the other hand, Focal Loss is designed to focus more on hard-to-classify pixels, thus improving the learning process for difficult areas within the image [32]. In our implementation, the total loss is calculated as follows:

$$Model\ Loss = Dice\ Loss + Focal\ Loss \quad (2)$$

After the last training, the evaluation metrics used to assess the performance of the models are reported in Table 1.

Among the various models evaluated, the Honeycombing model exhibits a need for further improvement, as it is comparatively less satisfactory than the other models, but it is sufficient for the detection and differentiation between the other types of defects. Its performance can be attributed to two primary factors. First, the challenge of acquiring a diverse set of images depicting honeycombed areas, the limited variability in the dataset hinders the model's ability to learn and generalize effectively. Second, the intrinsic variability within honeycombed areas themselves poses a significant challenge; these areas often exhibit considerable differences from one another in terms of size, shape, and texture, complicating the model's task of accurate identification and analysis.

To overcome these challenges, it is essential to enrich the dataset with a wider and more diverse range of images. This expansion would provide the model with a more complete understanding of the variations in honeycombing areas, thus improving its ability to accurately identify and analyse these defects. Improving the dataset is crucial to increasing the model's performance and ensuring its reliability in practical applications.

The output of the AI neural network is subsequently used to extract the features to be assessed.

The segmented image is represented in a binary format, where the background is white, and the black pixels indicate the object of interest. Using this binary delineation, the measurement of defect characteristics becomes simple. The specific features of interest for each defect type were established through a questionnaire conducted with construction companies, aligning the research with expert consensus, as summarised in Table 2.

The dimensions of the crack, i.e. width and length, are measured from the crack segmentation, which is enlarged so that the ROI includes the crack itself and only a small portion of the background surrounding it. The quantification process employs

Table 1. IoU score and model loss for the four models at the end of the training.

Defect Type	IoU score	Model loss
Crack	0.991	0.135
Pitting	0.993	0.029
Honeycombing	0.832	0.197
Exposed bar	0.978	0.140

Table 2. Defect features and reference units.

Defect Type	Features	Measurement unit
Crack	width and length	mm
Pitting	area	%
Honeycombing	area	mm ²
Exposed bar	width and length	mm

Steger's algorithm, which allows for sub-pixel resolution in the measurement of crack extension. This algorithm performs a colour analysis within the ROI to ascertain the contrast value, which determines a parameter that is iteratively used to calculate the crack width and length [33]–[35]. In Figure 4, the crack identified by the algorithm is shown.

Pitting areas are segmented by the AI model, allowing easy identification. The pitting measurement involves the calculation of the total pitting area and its ratio to the total image area to define the percentage value.

For honeycombing, the feature of interest is the total defected area, obtained by counting the number of pixels segmented by the AI model. A minimum value for the area to be considered as defect is set to 10 cm² to avoid false detection, which is usually due to small areas.

Exposed bars are evaluated by determining the width and length of the exhibited part of the bar. The segmented image is analysed to select the area corresponding to the exposed bar and the rectangle with the smallest area, surrounding the bar, is outlined. The width and length considered are the width and length of the rectangle.

As mentioned above, the measurements obtained are then converted from pixels to millimetres by means of a calibration carried out beforehand. An example of pitting, honeycombing, and exposed bar identification shown in Figure 5, with the measured features.

3.1.3. Quality Control interface for defect identification and measurement

The quality control system is equipped with a Graphical User Interface (GUI) to control the image acquisition devices, view

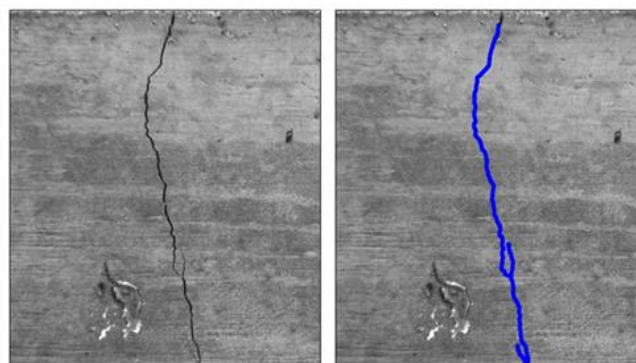


Figure 4. Crack identification: width: 0.32 mm, length: 143.01 mm.

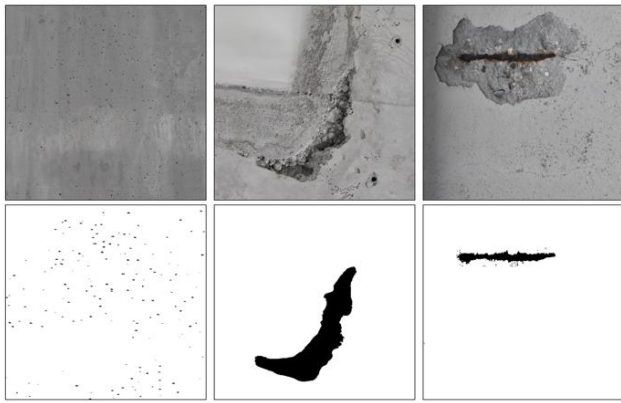


Figure 5. Pitting identification (left): percentage area: 0.14 %; honeycombing (middle): total defected area: 1251.6 mm²; exposed bar (right): width: 14.42 mm, length: 2.31 mm.

and analyse the acquired image, and display any defect types and characteristics. If a defect is detected, data can be sent to the digital platform directly from the interface (Figure 6).

The interface was implemented in Python and is currently compatible with Windows and Linux-based operating systems. The interface was designed for real-time quality control inspection, but it also accommodates retrospective analysis using previously acquired data.

In both scenarios, it allows to capture accurate data, which is then uploaded to the digital platform. The information obtained from the data, already processed by the AI-based algorithms, will be available for further inspection by the quality manager or the responsible person of the construction site. The data attributes conveyed to the platform include all the main information: domain, location, image, defect type, measured feature (depending on the defect type), timestamp and criticality value.

The steps are as follows:

1. **Load or acquire image:** the defect image to be processed can be an existing image in a local folder or can be acquired in real time through the connected cameras.

2. **Insert or acquire depth value:** the value can be already known or can be acquired in real time using the depth camera.
3. **Domain Specification:** in the context of this project, the domain indicates the specific building where the defect has been identified.
4. **Location:** insert the relative location of the defect among the building element, such as wall or column. The location data is stored as the position of the framed scene by the camera with respect to the entire element.
5. **Start the processing:** the image is processed by the models and algorithms previously defined to identify and classify the defects and measure their entity.
6. **Analyse the results:** the defect results, as segmented images and measured features, can be seen for each defect type identified, and the user can evaluate them before saving them.
7. **Insert the authentication token:** a JSON Web Token (JWT) must be entered to gain access to the platform and enter data; this step ensures data security [36].
8. **Save and send the results:** all relevant defect information is stored in a JSON file, which is sent to the platform to inject defect data.
9. **Connect the defect to the building element:** the IRI (Internationalized Resource Identifier) code of the element with defect can be fetched from the B2T dashboard, developed by the project partner CSTB [37], where the element of interest can be browsed and found. Using this code, a JSON file is created through which the connection between the previously injected defect and the element is generated on the DBT platform.

To increase the portability of the system, the graphical interface can be installed on a Windows tablet using an executable file.

3.2. How to integrate quality control in the digital platform?

The digital platform, Thing'in, which was developed by Orange [38], is primarily responsible for data management tasks.

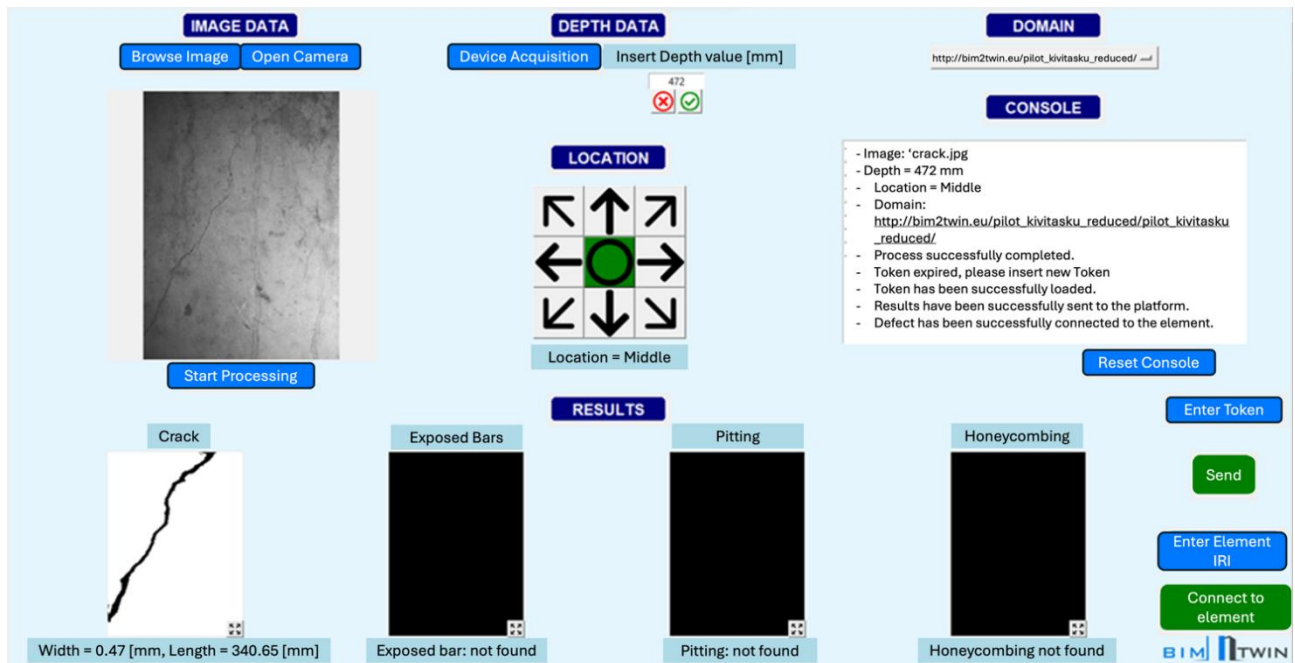


Figure 6. Quality control system user interface.

Various services can connect to the platform through its RestAPI to request up-to-date information regarding the digital twin and push newly gained knowledge, e.g., from analysing raw monitoring data, like images and sensor measurements.

Since the platform needs to manage information about construction processes, building elements, resources, and many other things that are strongly connected to each other, the digital platform is primarily based on a graph database.

The platform comprises many individual modules because it uses a microservice-based approach.

This paper only introduces the modules relevant to the quality control service.

3.2.1. Digital platform functionalities

A simplified overview of the digital platform developed in the frame of BIM2TWIN is presented in Figure 7.

The section in the middle represents the core data management modules, like the graph database, data validation, and conversion and injection components, which translate external data into the internally used data schema.

On the top are the external services, which connect to the platform through the RestAPI.

The connection between the services and the API is depicted with grey arrows. Depending on the construction project's requirements, a different set of services should be selected to adapt to the project's needs.

On the right-hand side, one can see the different types of data sources like project intent information originating from the planning phase and raw monitoring data collected on-site, which need to be fed into the platform.

Finally, the bottom shows the main dashboard, which can be viewed as a specific type of service. It requests information from the platform for visualization purposes. However, it does not update information on the platform.

o Data management

The data management module mainly comprises the underlying graph database. Besides standard graph database features (storage and querying), the digital platform API allows attaching files (Binary Large Objects or BLOBs) to individual graph nodes [38]. This can be useful, e.g., for connecting a defect image to the semantic description of the defect. The digital platform also includes the Ontology Lookup Service, which allows registering and using the data schema the instance graph must comply with, i.e. ontologies.

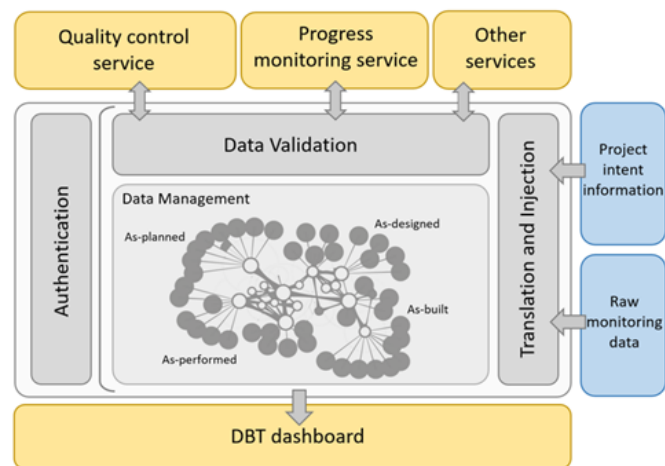


Figure 7. Digital platform architecture.

o Validation

The validation module checks all requests for data insertion or updates for compliance with the validation rules, to ensure that all the information added to the platform by various services is consistent. This ensures interoperability between multiple services and the possibility of profiting from each other. The validation rules are formulated with SHACL (Shapes Constraint Language) [39] and consider the correct domain and range of class attributes and relationships, according to the BIM2TWIN ontologies.

o RestAPI

The Thing'in platform already provides a generic RestAPI to request and manipulate graph nodes, edges, and attributes. On top of this generic API layer, a second API layer was developed, which groups commonly used sets of generic API calls into a single API request. This simplifies the integration of the services with the platform.

3.2.2. BIM2TWIN Ontologies

The BIM2TWIN Ontologies are ontologies developed in the frame of the BIM2TWIN project, specifically for digital twins of the construction phase.

They build upon the Building Topology Ontology (BOT) [40], which describes buildings and their components by their hierarchical and topological structure. These classes are extended with terminology to describe construction processes, resources, defects, and other objects relevant to Digital Twin Construction (DTC). While the BIM2TWIN Core Ontology includes generic classes that can be used independently of applied use cases, the BIM2TWIN Core Extension Ontology provides domain and use-case-specific details.

In the context of the quality control service of concrete surfaces, terms were added to the ontology to properly represent the concepts it covers. This contains classes, relationships, and attributes to describe surface defects with their parameters and assign them to specific building elements.

Figure 8 shows a UML diagram of the ontology, focusing on the relevant section for quality monitoring.

Two options are available for defining the position of defects. The first option specifies the absolute position of the defect through X, Y, and Z coordinates. The second option describes the relative position of the defect on the element, with predefined terms like top-right or bottom-left.

For more information regarding the BIM2TWIN Ontologies, the reader is referred to Schlenger et al. [41].

3.2.3. API Requirements and data integration

Images collected for defect assessment are automatically processed by the algorithms to extract defect classes and features. The data resulting from this analysis should then be entered into the digital platform (Figure 9).

The defect information added to the DBT platform, decided in collaboration with the partner of the project where the methodology was developed, is displayed in detail in Table 3. Some attributes are optional and/or defined for only some types of defects (Table 3). In fact, the standards related to defect evaluation do not specify a criticality except for crack defects.

During the first demonstration of the quality control service to the construction manager, a survey was submitted to obtain feedback on this topic. According to the construction managers, defects' criticality should be defined based on their geometric size (e.g., length and width for crack) in combination with the location of the building element of the defect, such as wall or column, and the relative position of the defect to the element.

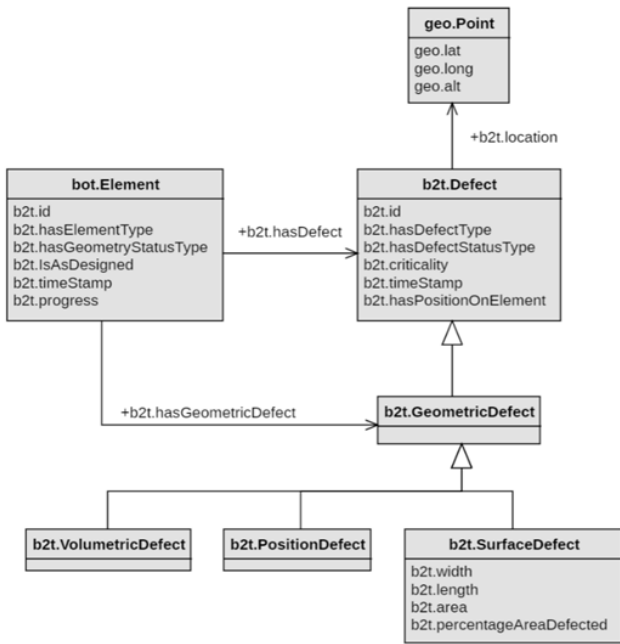


Figure 8. UML diagram of a section of the BIM2TWIN Core Extension Ontology showing defect-related classes.

Some defects, such as exposed bars and honeycombing are always defined as critical. The relative IRI and domain attributes are important from the integration point of view.

Each defect instance is added to the DBT platform as a node, connected to another node representing the building element. The defect node contains the main attributes necessary to describe the defect:

1. Domain: the namespace for the whole building twin;
2. IRI: Internationalized Resource Identifier, a unique identifier for each node;
3. Timestamp: the date and time in which the photo of the defect was acquired;
4. Defect type: the class of the defect, in this case the considered classes are crack, pitting, honeycombing, and exposed bar;
5. Defect features: the measured features depending on defect type, as explained in Section 3.1.2, optional;
6. Location: the relative position of the defect with respect to the building element (see Section 3.1.3), optional;
7. Defect status: pending or fixed;

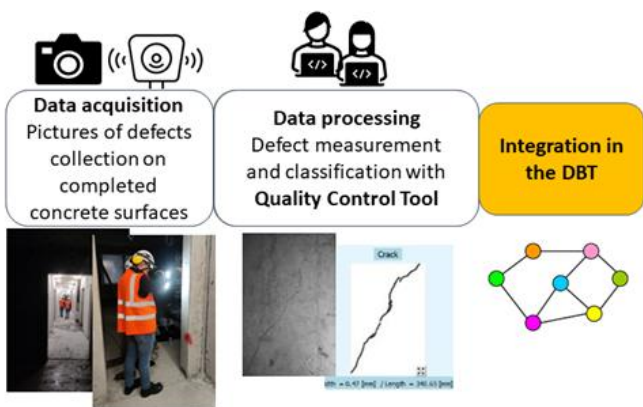


Figure 9. Quality control system dataflow: acquisition, processing, integration.

Table 3. Defect attributes and their respective constraints to be added to the DBT platform.

Defects Attributes	Constraints
Domain	Mandatory item
IRI	Mandatory item
Timestamp	Mandatory item
Defect type	Select: Crack, Exposed bars, Honeycombing, Pitting
Width in mm	Select: Crack or Exposed bars
Length in mm	Select: Crack or Exposed bars
Area in mm ²	Select: Honeycombing
Percentage of area %	Select: Pitting
Location	Select: See the pad in the interface.
Defect status	Mandatory item (pending or fixed)
Criticality	Mandatory item (from one to three)

8. Criticality: from one to three and defined in collaboration with the construction companies. As explained above, during the meeting session with managers, the feedback obtained was the following: the criticality value depends on the defect type; for exposed bars and honeycombing, it is set to three because they are always critical; for pitting, it is set to one because it is only an aesthetic defect; for cracks, the criticality level depends on the width:

- a. 1: if $w < 0.1$ mm
- b. 2: if $0.1 \text{ mm} < w < 0.3$ mm
- c. 3: if $w > 0.3$ mm.

The integration of the data into the DBT platform can be performed programmatically (through software) or using a REST client such as Postman, suggested by the partner [42]. Programmatically (e.g. in our case in Python), it is possible to make a series of API calls to obtain information and inject all data at once in the platform. The latter is in line with the functionality of Postman, but it introduces a programmable and automated dimension that is more efficient and reproducible.

The logical steps for the data injection are the same for both methods and are now explained to relate the collected element defect to the building components.

1. **get_Authorization_token**: Obtain a JWT from the platform for secure authentication in all subsequent steps.
2. **post_finished_Elements**: The finished elements, as-built elements, are fetched by the platform API by the IRI code of the element of interest.
3. **post_set_Defects**: The JSON file containing the information can be used to input the defect data extracted from the inspection software into the digital platform.
4. **post_connection_As_built**: This command allows the connection between the defect node and the as-built element node defined above.
5. **post_get_Elements_With_Defects**: To verify that the entire procedure was successful, this function is used to display the interconnection between the nodes.

4. APPLICATION TO A CONSTRUCTION USE CASE

4.1. The FIRA use case

In-situ acquisition and validation have been performed to demonstrate the efficiency of the quality control digital twin in operating conditions. The building selected is in Helsinki,

Finland, made available by the FIRA construction company. The monitoring toolkit described in Figure 2 was used, and the acquired defect images were analysed to consider the criticality level (Figure 10).

The acquisition was performed on one of the three parts of the entire building, on three floors, and in a total of 24 rooms of different sizes. In fact, it was an unfinished building, and not all the rooms and floors were accessible.

The illumination and temperature of the inspected environment are important conditions for the accuracy of the measurement. Therefore, the system is equipped with artificial light sources and battery charging systems to cope with hostile conditions.

4.2. Identified defects

The data acquired during the measurement campaign have been processed and analysed. Only three defect types were found: cracks, pitting, and honeycombing.

The measurement analysis is reported in Table 4 and Table 5. In particular, Table 4 summarizes the number of defects for each type; while in Table 5, the data are outlined according to the minimum, the maximum, and the mean value of each defect type, considering the features of interest for any defect type.

Most of the observed defects were labelled as pitting, in accordance with expectations, and due to the construction company's propensity to use prefabricated components in wall construction. Honeycombed areas were predominantly minor in extent.

Regarding cracks, most of them were classified as non-critical. An example of each defect type is shown in the following figures (Figure 11, Figure 12, Figure 13). In each figure the original defect image is placed on the left side, and the defect detected by the AI-based algorithm is on the right side. The measured features for each type of defect found are listed in the figure

Table 4. Number of defects found in FIRA building.

Defect Type	Number of defects found
Crack	9
Pitting	41
Honeycombing	7

Table 5. Measurements of defects features in FIRA building.

Defect Type	Features	Min value	Max value	Mean value	Units
Crack	width	0.17	1.22	0.6	mm
	length	2.15	340.65	168.46	mm
Pitting	area	0.18	1.49	0.61	%
Honeycombing	area	2258.27	27425.22	7596.67	mm ²

captions. The challenging aspect of this study is the correct recognition of the defect types; in fact, sometimes the recognition of exposed bars and cracks is hard to understand for

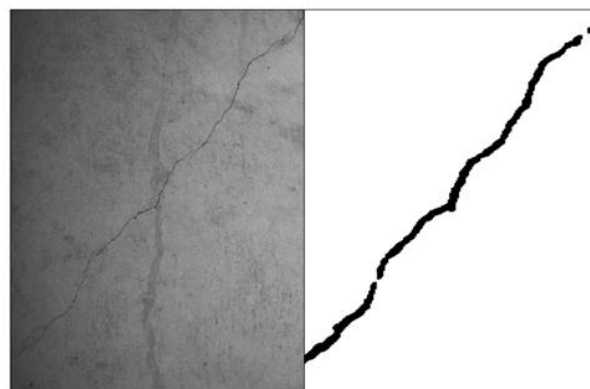


Figure 11. Image of a crack defect (left) and segmented crack (right). The features extracted for this defect are width: 0.47 mm and length: 340.65 mm.

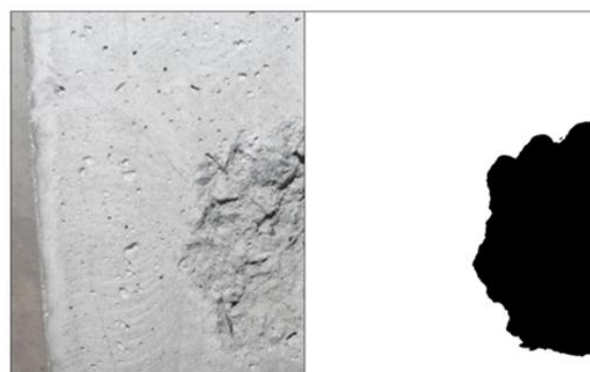


Figure 12. Image of a honeycombing defect (left) and segmented honeycombing (right). The features extracted for this defect is: area: 12066.58 mm².



Figure 13. Image of a pitting defect (left) and segmented pitting (right). The features extracted for this defect is: percentage area: 1.49 %.

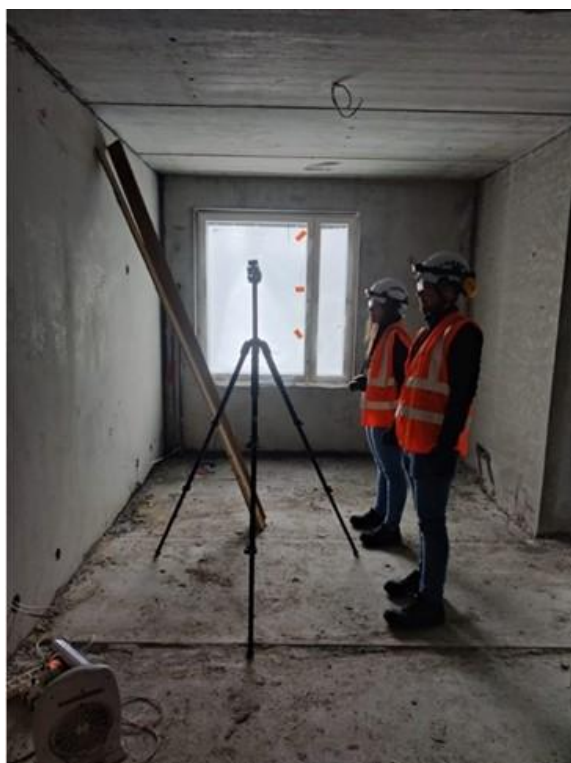


Figure 10. Quality control system installed in-situ under construction during the inspection.

the AI model, this is why improvements of the dataset are always on going to reduce the ambiguity of the identification, improving the training. The analysed data were integrated into the DBT platform in order to relate the defect to the element with discrepancies collected in the building.

4.3. Defect features visualization

A comprehensive dashboard was developed to improve the monitoring capabilities [43], and to allow the user to track all services simultaneously. It integrates a BIM framework, pre-processing and post-processing data, and the temporal evolution of the project data.

The dashboard contains a 3D progression of the building for each domain, in which the user can interactively select an individual element, and its information will be displayed (Figure 14).

For project managers, a salient function is the capability to trace patterns of defects. This option is not solely for cataloguing purposes, but it also serves as a diagnostic tool to infer potential causes. The functionalities include the enumeration of defects by various defect types and locations, specifically floors or rooms, and the aim is to obtain a distribution, thus facilitating decision-making processes.

5. DISCUSSION

This work aimed to carry out a non-destructive analysis and inspection on surface defects present on concrete structures, using vision systems and AI algorithms, to obtain an output to be introduced into a digital building model to monitor the health of the building during its life stages. This activity is related to a project that aims to create a Digital Building Twin (DBT) platform for construction management that implements lean

principles to reduce operational waste of all kinds, shorten times, reduce costs, improve quality and safety, and reduce the carbon footprint, as designed in [37] and [38] for data entry in this case of the extent of defects.

This involved a state-of-the-art study regarding the digital twin and the AI currently used for defect analysis.

The vision system has been properly selected and calibrated for the application. Geometric functions have been defined for the quantification of the defect's type. An AI architecture and metrics were selected for the model's generation. Finally, a measurement campaign has been conducted to analyse the defects that may occur during the construction stage of a building. FIRA, a construction company partner in the European BIM2TWIN project, made available a building for few days in January 2023, to collect images both for the extension of the specific dataset, which had already been previously created, and for the validation of the measurement algorithms developed.

As a result, the defects' information and features have been obtained and injected in the digital platform with the images. This data can be used to understand the severity of defects on each element, and can be used by other partners to compute alternative plans to continue the work with the best of these[43], [44]. In fact, the presence of a defect may cause a delay if it needs to be fixed, but this intervention during construction will reduce the maintenance time that can occur in the future.

The proposed computer vision methods exhibit some problematic aspects, which are detailed as follows. A critical variable during the image acquisition phase is the ambient light source. Neural networks, crucial in this process, are often affected by uncertainties. These uncertainties are mainly due to the complexity of the dataset, stemming from environmental variability where the target image is captured compared to the

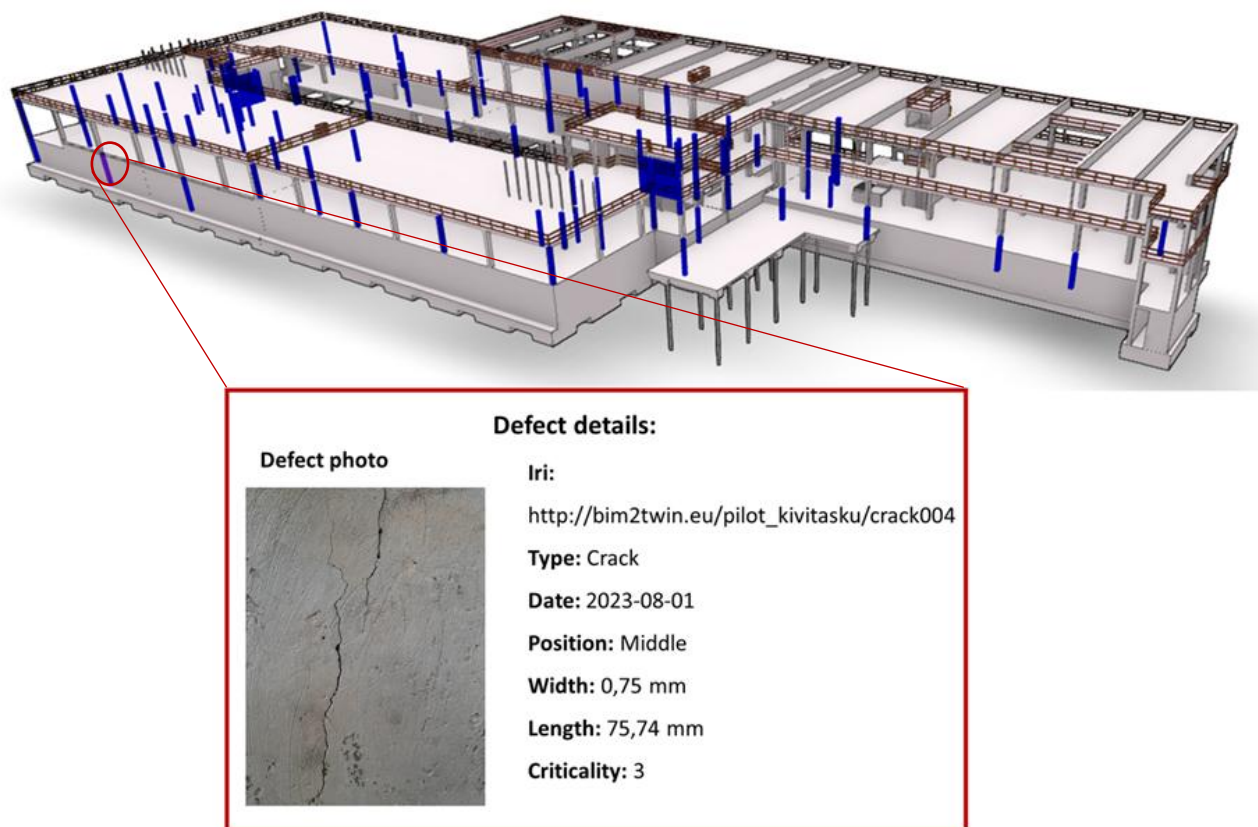


Figure 14. Defect information visualization on dashboard.

trained image. In terms of defect identification, challenges arise with the identification of honeycombing, as mentioned in Section 3.1.2.

6. CONCLUSION

The presented method identifies, classifies, and measures defects while maintaining a trade-off between portability and the responsiveness of user interface that is a great step forward from the literature. In fact, using 2D images the computational load is reduced, and the reactivity of the system can be considered acceptable. The BIM2TWIN construction partners of the project rate this approach as quite responsive. The portability of the system was considered in order to be able to easily use the service even on building sites with a tablet and the previously presented sensors installed on it. By combining this service with the dashboard, the location of the defect on the building can be identified by entering the element IRI on which the defect is located and linking the defect and its features to the building element with the presented approach, allowing in this way a direct data injection into the DBT platform.

Future studies will be conducted on improving the defect detection method for the identification and quantification of the defect entities, e.g., by testing different neural network architectures and also different materials on which to apply defect detection. A study on defect detection on masonry surfaces has already been conducted with satisfactory results [45].

AUTHORS' CONTRIBUTION

Maria Teresa Calcagni: conceptualization, methodology, software, investigation, data curation, writing (original draft).

Giovanni Salerno: conceptualization, methodology, software, investigation, data curation, writing (original draft).

Milena Martarelli: conceptualization, investigation, resources, writing (review & editing), supervision.

Jonas Urs Schlenger: conceptualization, methodology, software, investigation, data curation, writing (original draft).

Thomas Hassan: software, resources, writing (review & editing).

Rene Heinikainen: resources, writing (review & editing).

André Borrmann: resources, writing (review & editing), supervision, project administration, funding acquisition.

Bruno Fies: resources, project administration, funding acquisition.

Gian Marco Revel: resources, supervision, project administration, funding acquisition.

ACKNOWLEDGEMENT

The research presented in this paper has been funded by the European Union's Horizon 2020 research and innovation programme under grant agreement no. 958398, "BIM2TWIN: Optimal Construction Management & Production Control".

REFERENCES

- [1] C. Z. Dong, F. N. Catbas, A review of computer vision-based structural health monitoring at local and global levels, *Structural Health Monitoring* 20(2) (2021), pp. 692–743.
- [2] H. J. Kohoutek, Intelligent instrumentation: a quality challenge, *Acta IMEKO* 3(1) (2014)
DOI: [10.21014/acta_imeko.v3i1.195](https://doi.org/10.21014/acta_imeko.v3i1.195)
- [3] L. Morero, F. Visone, N. Abate, A. M. Amodio, M. Prodomo, M. Sileo, N. Masini, The use of a Heritage Building Information Model as an effective tool for planning restoration and diagnostic activities: the example of the Troia Cathedral rose window, *Acta IMEKO* 12(4) (2023).
DOI: [10.21014/actaimeko.v12i4.1511](https://doi.org/10.21014/actaimeko.v12i4.1511)
- [4] D. D. Eneyew, M. A. M. Capretz, G. T. Bitsuamlak, Toward Smart-Building Digital Twins: BIM and IoT Data Integration, *IEEE Access* 10 (2022), pp. 130487–130506.
DOI: [10.1109/ACCESS.2022.3229370](https://doi.org/10.1109/ACCESS.2022.3229370)
- [5] K. Zhang, C. Wang, Y. Zhao, J. Bi, Experimental study on cracking behavior of concrete containing hole defects, *Journal of Building Engineering* 65 (2023), art. no. 105806.
DOI: [10.1016/j.jobbe.2022.105806](https://doi.org/10.1016/j.jobbe.2022.105806)
- [6] M. Hong, D. Lei, F. Hu, Z. Chen, Assessment of void and crack defects in early-age concrete, *Journal of Building Engineering* 70 (2023) art. no. 106372.
DOI: [10.1016/j.jobbe.2023.106372](https://doi.org/10.1016/j.jobbe.2023.106372)
- [7] F. Rodríguez, W. D. Chicaiza, A. Sánchez, J. M. Escaño, Updating digital twins: Methodology for data accuracy quality control using machine learning techniques, *Computers in Industry* 151 (2023), art. no. 103958.
DOI: [10.1016/j.compind.2023.103958](https://doi.org/10.1016/j.compind.2023.103958)
- [8] Scribd, Types and Causes of Concrete Deterioration Is536 PDF | PDF | Corrosion | Reinforced Concrete, Scribd. Online [Accessed 22 August 2025]
<https://www.scribd.com/document/375196995/types-and-causes-of-concrete-deterioration-is536-pdf>
- [9] B. G. Pantoja-Rosero, R. Achanta, K. Beyer, Damage-augmented digital twins towards the automated inspection of buildings, *Automation in Construction* 150 (2023), art. no. 104842.
DOI: [10.1016/j.autcon.2023.104842](https://doi.org/10.1016/j.autcon.2023.104842)
- [10] V. Fioriti, A. Cataldo, A. Colucci, C. Ormando, F. F. Saitta, D. Palumbo, I. Roselli, Innovative graph-based video processing methodology for collapse early warning of historic masonry buildings, *Acta IMEKO* 13(2) (2024)
DOI: [10.21014/actaimeko.v13i2.1756](https://doi.org/10.21014/actaimeko.v13i2.1756)
- [11] B. F. Spencer, V. Hoskere, Y. Narazaki, Advances in Computer Vision-Based Civil Infrastructure Inspection and Monitoring, *Engineering* 5(2) (2019), pp. 199–222.
DOI: [10.1016/j.eng.2018.11.030](https://doi.org/10.1016/j.eng.2018.11.030)
- [12] J. K. Chow, Z. Su, J. Wu, Z. Li, P. S. Tan, K. Liu, X. Mao, Y. H. Wang, Artificial intelligence-empowered pipeline for image-based inspection of concrete structures, *Automation in Construction* 120 (2020), art. no. 103372.
DOI: [10.1016/j.autcon.2020.103372](https://doi.org/10.1016/j.autcon.2020.103372)
- [13] H. Zoubir, M. Rguig, M. El Aroussi, A. Chehri, R. Saadane, G. Jeon, Concrete Bridge Defects Identification and Localization Based on Classification Deep Convolutional Neural Networks and Transfer Learning, *Remote Sensing* 14(19) (2022)
DOI: [10.3390/rs14194882](https://doi.org/10.3390/rs14194882)
- [14] W. Wang, C. Su, D. Fu, Automatic detection of defects in concrete structures based on deep learning, *Structures* 43 (2022), pp. 192–199.
DOI: [10.1016/j.istruc.2022.06.042](https://doi.org/10.1016/j.istruc.2022.06.042)
- [15] K. Sarkar, A. Shiuly, K. G. Dhal, Revolutionizing concrete analysis: An in-depth survey of AI-powered insights with image-centric approaches on comprehensive quality control, advanced crack detection and concrete property exploration, *Construction and Building Materials* 411 (2024), art. no. 134212.
DOI: [10.1016/j.conbuildmat.2023.134212](https://doi.org/10.1016/j.conbuildmat.2023.134212)
- [16] M. Dang, H. Wang, TH Nguyen, L. Tightiz, L. D. Tien, T. N. Nguyen, N. P. Nguyen, CDD-TR: Automated concrete defect investigation using an improved deformable transformers, *Journal of Building Engineering* 75 (2023), art. no. 106976.
DOI: [10.1016/j.jobbe.2023.106976](https://doi.org/10.1016/j.jobbe.2023.106976)
- [17] G. Ye, J. Qu, J. Tao, W. Dai, Y. Mao, Q. Jin, Autonomous surface crack identification of concrete structures based on the YOLOv7 algorithm, *Journal of Building Engineering* 73 (2023), art. no. 106688.
DOI: [10.1016/j.jobbe.2023.106688](https://doi.org/10.1016/j.jobbe.2023.106688)

- [18] W. Wang, C. Su, Automatic classification of reinforced concrete bridge defects using the hybrid network, Arab J Sci Eng 47(4) (2022), pp. 5187–5197.
DOI: [10.1007/s13369-021-06474-x](https://doi.org/10.1007/s13369-021-06474-x)
- [19] J. K. Chow, K. Liu, P. S. Tan, Z. Su, J. Wu, Z. Li, Y. H. Wang, Automated defect inspection of concrete structures, Automation in Construction 132 (2021), art. no. 103959.
DOI: [10.1016/j.autcon.2021.103959](https://doi.org/10.1016/j.autcon.2021.103959)
- [20] S. E. Park, S.-H. Eem, H. Jeon, Concrete crack detection and quantification using deep learning and structured light, Construction and Building Materials 252 (2020), art. no. 119096.
DOI: [10.1016/j.conbuildmat.2020.119096](https://doi.org/10.1016/j.conbuildmat.2020.119096)
- [21] Y. Zhao, J. Yu, W. Jin, Damage analysis and cracking model of reinforced concrete structures with rebar corrosion, Corrosion Science 53(10) (2011), pp. 3388–3397.
DOI: [10.1016/j.corsci.2011.06.018](https://doi.org/10.1016/j.corsci.2011.06.018)
- [22] X. Han, Z. Zhao, L. Chen, X. Hu, Y. Tian, C. Zhai, L. Wang, X. Huang, Structural damage-causing concrete cracking detection based on a deep-learning method, Construction and Building Materials 337 (2022), art. no. 127562.
DOI: [10.1016/j.conbuildmat.2022.127562](https://doi.org/10.1016/j.conbuildmat.2022.127562)
- [23] Gonzalo, Concrete cracks and concrete fissures | Deterioration, BECOSAN®. Online [Accessed 22 August 2025]
<https://www.becosan.com/concrete-cracks-concrete-fissures/>
- [24] Level Best, Concrete Pitting: Causes, Prevention, and Repair — Level Best, LLC. Online [Accessed 22 August 2025]
<https://www.levelbestohio.com/blog/concrete-pitting-causes-prevention-and-repair>
- [25] UltraTech Cement, What is Honeycombing of Concrete? Causes and Types, UltraTech Cement. Online [Accessed 22 August 2025]
<https://www.ultratechcement.com/for-homebuilders/home-building-explained-single/descriptive-articles/honeycombing-in-concrete#>
- [26] JLC, Troubleshooting: Exposed Reinforcing Steel, Concrete Construction. Online [Accessed 22 August 2025]
https://www.concreteconstruction.net/how-to/repair/troubleshooting-exposed-reinforcing-steel_o
- [27] Nikon, Nikon D7200 Low-Light DSLR with Built-in WiFi, NFC & More. Online [Accessed 22 August 2025]
<https://www.nikonusa.com/p/d7200/1554/overview>
- [28] Intel, Intel® RealSense™ LiDAR Camera L515, Intel® RealSense™ Depth and Tracking Cameras. Online [Accessed 22 August 2025]
<https://www.intelrealsense.com/lidar-camera-l515/>
- [29] W. Wang, C. Su, Automatic concrete crack segmentation model based on transformer, Automation in Construction 139 (2022), art. no. 104275.
DOI: [10.1016/j.autcon.2022.104275](https://doi.org/10.1016/j.autcon.2022.104275)
- [30] O. Ronneberger, P. Fischer, T. Brox, U-Net: Convolutional Networks for Biomedical Image Segmentation, in Medical Image Computing and Computer-Assisted Intervention – MICCAI 2015, N. Navab, J. Hornegger, W. M. Wells, and A. F. Frangi, Eds., Cham: Springer International Publishing, 2015, pp. 234–241.
DOI: [10.1007/978-3-319-24574-4_28](https://doi.org/10.1007/978-3-319-24574-4_28)
- [31] S. Jadon, A survey of loss functions for semantic segmentation, in 2020 IEEE conference on computational intelligence in bioinformatics and computational biology (CIBCB), IEEE, 2020, 27-29 October 2020, Via del Mar, Chile
DOI: [10.1109/CIBCB48159.2020.9277638](https://doi.org/10.1109/CIBCB48159.2020.9277638)
- [32] P. Yakubovskiy, Segmentation models documentation. 2021. Online [Accessed 22 August 2025].
<https://media.readthedocs.org/pdf/segmentation-models/latest/segmentation-models.pdf>
- [33] C. Steger, An unbiased detector of curvilinear structures, IEEE Transactions on Pattern Analysis and Machine Intelligence 20(2) (1998), pp. 113–125.
DOI: [10.1109/34.659930](https://doi.org/10.1109/34.659930)
- [34] N. Giulietti, P. Chiariotti, G. M. Revel, Automated measurement of geometric features in curvilinear structures exploiting Steger’s algorithm, Sensors 23(8) (2023), art. no. 4023.
DOI: [10.3390/s23084023](https://doi.org/10.3390/s23084023)
- [35] G. Cosoli, M. T. Calcagni, G. Salerno, A. Mancini, G. Narang, A. Galdelli, A. Mobili, F. Tittarelli, G. M. Revel, In the direction of an artificial intelligence-enabled monitoring platform for concrete structures, Sensors 24(2) (2024), art. no. 2:
DOI: [10.3390/s24020572](https://doi.org/10.3390/s24020572)
- [36] JWT, JWT.IO. Online [Accessed 22 August 2025]
<http://jwt.io/>
- [37] D2.1 – Digital Building Twin Requirements - Analysis and Data Model, Project Report [Accessed 22 August 2025]
https://bim2twin.eu/wp-content/uploads/2022/10/Attachment_D2.1.pdf
- [38] Orange, thing_in_whitepaper.pdf Online [Accessed 22 August 2025]
https://www.thinginthefuture.com/IMG/pdf/thing_in_whitepaper.pdf
- [39] W3C, Shapes Constraint Language (SHACL). Online [Accessed 22 August 2025]
<https://www.w3.org/TR/shacl/>
- [40] M. H. Rasmussen, M. Lefrançois, G. Schneider, P. Pauwels, BOT: the building topology ontology of the W3C linked building data group, Semantic Web 12(1) (2020), pp. 143–161.
DOI: [10.3233/SW-200385](https://doi.org/10.3233/SW-200385)
- [41] J. Schlenger, T. Yeung, S. Vilgertshofer, J. Martinez, R. Sacks, A. Borrmann, A comprehensive data schema for digital twin construction, Proc. of the 29th EG-ICE Int. Workshop on Intelligent Computing in Engineering, Aarhus, Denmark, 6-8 July 2022. Online [Accessed 22 August 2025]
<https://mediatum.ub.tum.de/doc/1689026/document.pdf>
- [42] Postman, ‘REST Client - Postman API Platform’, Postman API Platform. Online [Accessed 22 August 2025]
<https://www.postman.com/product/rest-client/>
- [43] J. Martinez, T. Yeung, R. Sacks, Production planners’ scope of action in the context of digital twin construction, The Twelfth Int. Conf. on Construction in the 21st Century (CIIC-12), Amman, Jordan, 16-19 May 2022. Online [Accessed 22 August 2025].
<https://bim2twin.eu/wp-content/uploads/2022/11/Production-Planners-Scope-of-Action-in-the-Context-of-Digital-Twin-Construction.pdf>
- [44] T. Yeung, J. Martinez, L.-O. Sharoni, R. Sacks, The Role of Simulation in Digital Twin Construction, Proc. of the 29th EG-ICE Int. Workshop on Intelligent Computing in Engineering, Aarhus, Denmark, 6-8 July 2022, p. 258.
DOI: [10.7146/aul.455.c215](https://doi.org/10.7146/aul.455.c215)
- [45] G. Salerno, M. T. Calcagni, M. Martarelli, G. M. Revel, Metrological evaluation of an AI-based vision computing model for crack detection on masonry structures, Proceedings of SUBLime Conference 2024 – Towards the Next Generation of Sustainable Masonry Systems: Mortars, Renders, Plasters and Other Challenges, 11-12 November 2024, Funchal, Madeira, Portugal, 403 (2024), art. no. 04002.
DOI: [10.1051/mateconf/202440304002](https://doi.org/10.1051/mateconf/202440304002)